Supplementary Materials

1. Compatible Street Configurations

The different zones outlined in Section 2.1.1 of the main text (receptor, emissions, neutral) permit a wide range of streets to be 'drawn' in the UI, and for the air quality code to calculate concentration changes across the street cross section. There are, however, a limited number of rules on where such zones can be located within the street, and where barriers can be placed therein. These rules allow what the authors believe to be the most common types of street configuration, while still enabling quick and robust results to be returned to the UI. The following rules apply:

- Receptor zones (RZ[X]) can only be located between the building and the Kerb on either side of the street. Note, 'Kerbs' referred to in this context are simply markers, used to check whether the user-specified configuration of zones is compatible with the air quality code; they do not necessarily represent physical kerbs that are accompanied by changes in grade. This emulates where most receptors are likely to spend significant periods of time; on pavements, front gardens, or other public spaces such as outdoor dining and seating areas. While receptors may cross an emission zone, it is unlikely that they will spend much time doing so, and therefore their exposure is expected to be short-lived. At least one receptor zone or neutral zone must lie between the Kerb and Street Boundary on both sides of the street, i.e., the distance between the Street Boundary and Kerb cannot be set to zero.
- Receptor zones attached to a building on either side of the street (RZBL[X]) represent areas of private ownership, such as front gardens. It is important to mark the distinction between the public and private land ownership, as the range of implementations and accountability for cost will differ between the two. It is possible for the user to set the width of either (or both) RZBL[X] zone(s) to be equal to zero if the façade of building 1 or 2 marks the Street Boundary. In this case, the air quality model assigns a width of 0.01 m to ensure that no two reference points are in the same location (e.g., street boundary and total road width) as this can impact the column dimensioning rules outlined below. In limited circumstances, this can lead to narrow column(s) at the left- or right-most edges, but this methodology ensures numerical stability of the solver discussed in SM section 7.
- Emission zones (EZ[X]) can only be located between the two Kerbs. At present, the number of emission zones is limited to a maximum of two and minimum of one.
- Neutral zones (NZ[X]) can be of any width and can be placed anywhere in the street cross section between both Street Boundaries. There is no maximum or minimum limit on the total number of neutral zones in the cross-section.
- Existing barriers may only be located within receptor zones attached to buildings (RZBL[X]'s), and are defaulted to lie at the edge of the zone, i.e., the Street Boundary. This is akin to a garden wall or fence which typically lies at the boundary to a property, marking the distinction between public and private land. A maximum of two existing barriers are permitted (one at each edge of each RZBL[X] zone) and are currently limited to 'grey' barriers with a user-defined obstruction value. There is no minimum number of existing barriers required for a result to be returned to the UI.
- A GI4RAQ barrier can be placed within either a receptor zone or neutral zone, but must be located between the Street Boundary and the Kerb (i.e. within the public realm) on one side of the street. If the middle of the GI4RAQ barrier is specified to be located at 0 m within the zone (i.e., at the left most edge), 0.01 m is added to the barrier's location. Alternatively, if the

middle of the GI4RAQ barrier is equal to the full width of the zone (i.e., at the right most edge), 0.01 m is subtracted from the barrier's location. These adjustments are made to ensure there are no two reference points in the same location (e.g., middle of GI4RAQ barrier and street boundary), as this could otherwise impact on the column dimensioning rules outlined below.

The simplest street configuration is outlined in Figure S1; two buildings of equal height, one receptor zone attached to each building on either side of equal width, one receptor zone between the Street Boundary and Kerb on both sides, one emission zone, no neutral zones, no existing barriers, and the GI4RAQ barrier is in the middle of a receptor zone.

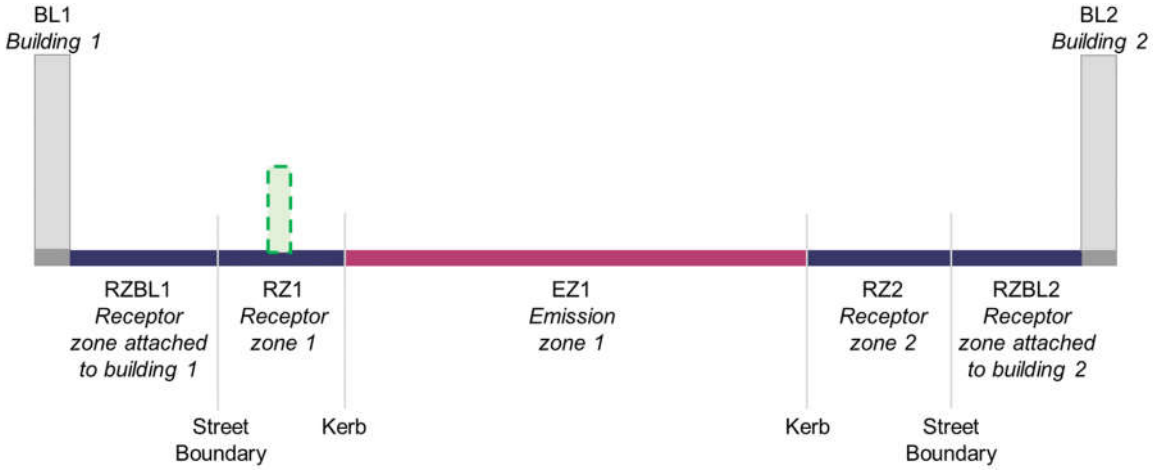

Figure S1 Example of simplistic street configuration

In comparison, a more complex street configuration is outlined in Figure S2; two buildings of different heights, RZBL1 set to 0m in width while RZBL2 has a positive width, a mix of receptor zones and neutral zones between the Street Boundary and Kerbs on both sides of the street, two emission zones adjoined by neutral zones between both Kerbs, an existing barrier on the right-hand side of the street, and a GI4RAQ barrier proposed on the left-hand side of the street.

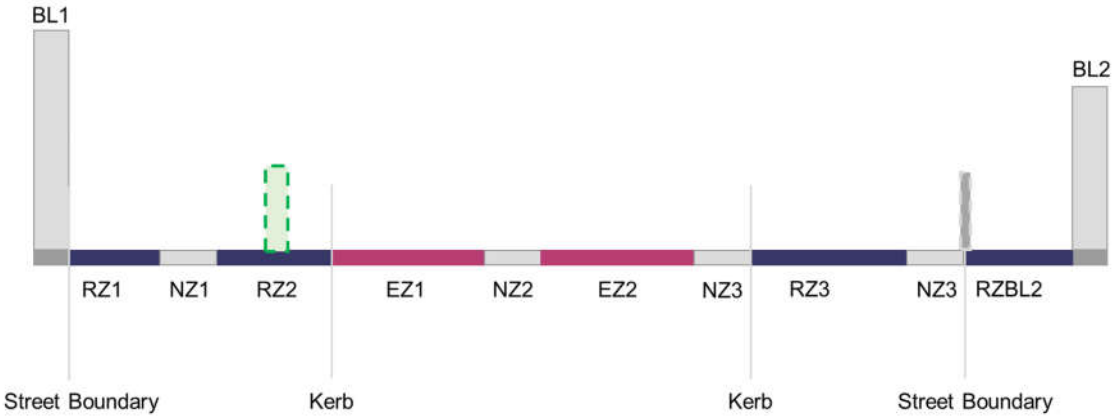

Figure S2 Example of complex street configuration. Note: within the air quality code the width of RZBL1 is defaulted to 0.01 m

2. Column Dimensioning

As outlined in section 2.1.2 of the main text, the dimensioning of the street cross-section into columns is completed with the aim to distinguish between regions where significant variations in concentrations are expected, as gradients within the boxes cannot be resolved. Distinguishing between air within the recirculation region and ventilation region, and subsequently how this relates to the reference locations outlined above, provides the upper-most criteria. Hence, there are six scenarios which govern how the street is dimensioned:

1. If the upwind building recirculation region extends up to but not including the upwind street boundary (<), the columns are dimensioned according to Figure S3 (within SI attachment folder).
2. If the upwind building recirculation region falls between the upwind street boundary (>=) and the start of the first emission zone (<), the columns are dimensioned according to Figure S4 (within SI attachment folder).
3. If the upwind building recirculation region falls between the start of the first emission zone (>=) and the downwind far edge of the last emission zone (<), the columns are dimensioned according to Figure S5 (within SI attachment folder).
4. If the upwind building recirculation region falls between the furthest edge of the last emission zone (>=) and the downwind street boundary (<), the columns are dimensioned according to Figure S6 (within SI attachment folder).
5. If the upwind building recirculation region falls between the downwind street boundary (>=) and the total street width (<), the columns are dimensioned according to Figure S7 (within SI attachment folder).
6. If the upwind building recirculation region fills the entire cross-section (>= the total street width) the columns are dimensioned according to Figure S8 (within SI attachment folder).

Figures S3-S8 refer to PDF files within the SI folder. Due to the size of the flow charts outlining the automatic dimensioning logic in each of the six cases above, it is not possible to display them all clearly within this single document.

3. Climatological wind conditions

The background climatological wind conditions above the street in question are used to drive patterns of air flow within the street, and the frequency with which they occur is used to weight overall results. Observed wind data is drawn upon from 15 meteorological stations across the UK, of which the nearest to the street in question (as the crow flies) is determined and corresponding data loaded into the air quality code. The stations are those that the UKMO use to characterise UK regional climates [71] and whose data are freely available from the Met Office Integrated Data Archive System (MIDAS) Open archive at the Centre for Environmental Data Analysis [45]; this archive is designated as public sector information, provided under an Open Government Licence (www.nationalarchives.gov.uk/doc/open-government-licence/version/3/).

The frequency of climatological wind conditions above the street in question is broken down into four categories: 1) wind blowing from left to right relative to the street axis, 2) wind blowing from right to left relative to the street axis, 3) wind blowing along the street axis (parallel) 'into' the plane of the street section, and 4) wind blowing parallel to the street 'out of' the plane of the street section, as identified in Figure S9. 'Slack' conditions that occur when the wind speed is below the detection limit of anemometers are assigned a wind speed of 0.5 ms^{-1}, and assumed to fall within the $U_{P,out}$ category. This ensures dispersion due to a low wind speed is still accounted for, but no recirculation region is prescribed.

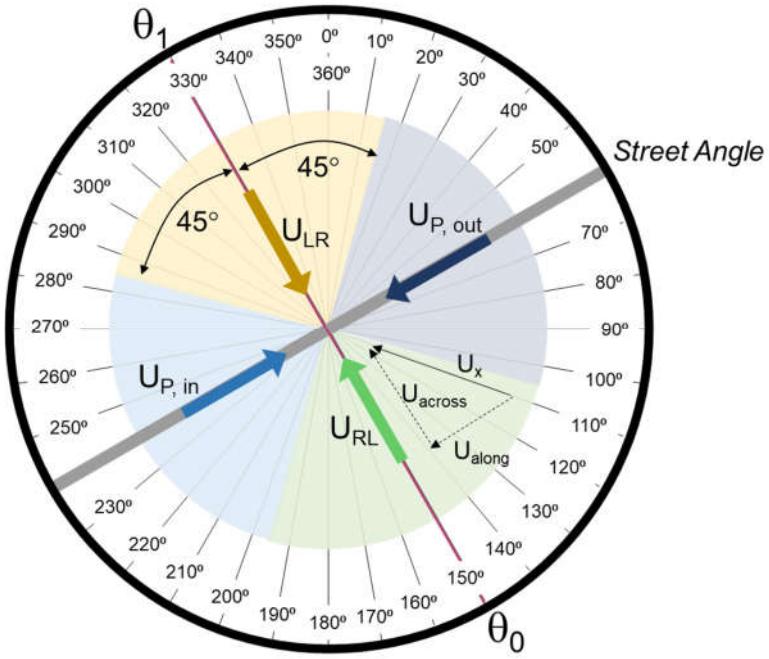

Figure S9 Schematic diagram to illustrate how perpendicular and parallel wind speeds are calculated from the background meteorological data

The mean observed background wind speed values are determined for each of the four cases. For cases (1) and (2) this is completed by identifying the perpendicular wind directions relative to the street axis (θ_0, θ_1), as shown in Figure S9. The across-street vector components (U_{across}) for each wind direction (U_x) ±45° from θ_0 and θ_1 is calculated using trigonometry. In this example, U_{LR} (when BL1 is rendered 'upwind') is calculated from the across-street components of wind vectors at 290° through to 10° and weighted based on each individual wind direction's frequency of occurrence. Conversely, U_{RL} (when BL2

is rendered 'upwind') is calculated as a weighted mean of the across-street wind components from 110^0 through to 190^0. A similar process is used to calculate the mean wind speed parallel to the street for cases (3) and (4); the along-street components of each wind vector ±45° from the street axis are determined and a weighted mean calculated based on magnitude and frequency of the wind vector. Parallel conditions represent the same physical processes irrespective of whether the wind direction is into or out of the plane of the street. Therefore, an overall weighted parallel wind speed is calculated (U_P).

The total frequency of wind conditions U_{LR}, U_{RL}, and U_P are checked to ensure they total 100% of wind conditions observed at the nearest meteorological station. Subsequently, our pairs of scenarios are simulated in the air quality model:

1. Where U_{LR} determines the magnitude and pattern of air flow in the street cross section, applied to the grid dimensioning determined when BL1 is rendered upwind, both with and without the proposed GI4RAQ barrier.
2. Where U_{RL} determines the magnitude and pattern of air flow in the street cross section, applied to the grid dimensioning determined when BL2 is rendered upwind, both with and without the proposed GI4RAQ barrier.
3. Where U_P determines exchange velocities (see SM section 6) across the model grid, as dimensioned when BL1 is rendered upwind, both with and without the proposed GI4RAQ barrier.
4. Where U_P determines exchange velocities (see SM section 6) across the model grid, as dimensioned when BL2 is rendered upwind, both with and without the proposed GI4RAQ barrier.

The percentage changes in pollutant concentrations within each pair of scenarios is calculated, and a weighted average percentage change for each box calculated based on the frequency of occurrence of U_{LR}, U_{RL}, and U_P. The frequency of U_P is split equally across scenarios (3) and (4). In cases where the dimensioning under U_{LR} and U_{RL} do not correspond to the same street locations, every column is preserved, and an area-weighted average percentage change calculated.

Note: U_{LR} and U_{RL} are subsequently referred to in SM section 5 as the time-averaged perpendicular component of the wind velocity when the wind blows within 45^0 of normal to the street, $\overline{u_{obs}}$. As U_{LR}, U_{RL} and U_P are calculated from observations at a meteorological station in relatively unobstructed terrain and at a height of 10 m, they are subsequently adjusted to determine wind speeds in an urban environment at any specified height, as described in SM section 5.

4. **Example street: flow and dimensioning under perpendicular wind blowing right to left**

As outlined in the main text, the column dimensions and resulting air flow is described by the model under each perpendicular wind condition. Figure S10 illustrates the model grid applied to our example street section when the wind aloft instead blows from right to left. The rows remain unchanged from the left-to-right perpendicular wind scenario (see Figure 3 and accompanying text in section 2.1.2 of the main paper) but the dimensioning of the columns differs. BL2 now lies upwind of the road relative to the wind aloft, and C4 and C5 are now used to resolve the circulation of air within its recirculation region, bringing air with emissions from the right hand end of EZ2 towards receptors in RZ2 and RZBL2. In the absence of an existing barrier at the right hand street boundary, C4 and C5 are divided in line with the proposed barrier (the dashed green rectangle); see SM section 2 for dimensioning in response to all permutations and combinations of existing and proposed barriers. The air flow inside a recirculation region is characterised by much lower advection velocities, than the air flow outside (see, e.g., [41]). We therefore do not attempt to simulate the diversion of air around a proposed barrier therein (saving a column in the process) and, instead, simply reduce the mixing of air between the boxes either side of it; see SM section 6. With three columns remaining, the left hand edge of C3 is aligned with the left hand edge of EZ1, to avoid artificially spreading out the emissions from EZ1 and EZ2, and C1 and C2 are used to differentiate between the regions in the private and public realms, either side of the left hand street boundary. The black arrows in Figure S10 indicate the directions (but not the magnitudes) of the advection velocities invoked to simulate the flow of air; the exchange velocities used to describe the slow mixing of air between adjacent boxes are not shown.

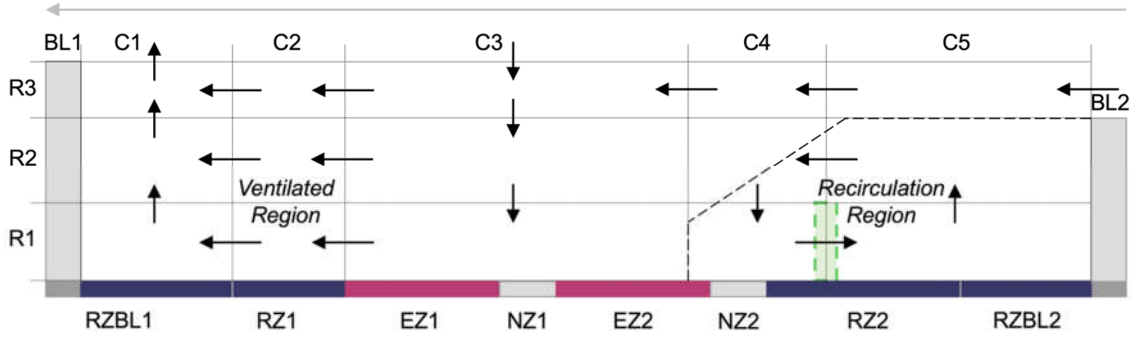

Figure S10 Model grid adopted to represent our example street section when the wind aloft blows from right to left, comprising five columns (C1-5) and three rows (R1-3). The black arrows indicate the directions (but not the magnitudes) of the advection velocities used to simulate the flow of air in the absence of the proposed barrier (the dashed green rectangle), and modified in response to it.

5. Estimating advection velocities

The flow of air into, around, and out of the user-specified street section is described by advection velocities at the interfaces between our 15 model boxes. We estimate advection velocities for each box edge in the perpendicular wind scenarios (i.e., left to right and right to left) based on the principle of air mass conservation (i.e. continuity equation of air mass). All advection velocities at box edges coincident with the edge of buildings, or the ground, are set to zero, as are all advection velocities under parallel and slack wind scenarios. The methodology outlined here is just one simple approach to estimate the wind speeds above an urban array and the values of advection velocities within the ventilated region of the street. This may be substituted with results from other methods such as CFD simulations in specific case studies. The different treatment of advection velocities within the recirculation region is subsequently outlined.

To estimate the values of the (non-zero) advection velocities in the ventilated region, we start by identifying the nearest UK Meteorological Office (UKMO) station to the location of that street section, and calculate the weighted-average across-street wind vector as described in SM section 3 (U_{LR} and U_{RL}). Assuming a neutral atmosphere and logarithmic wind profile [42], this observed perpendicular wind speed, $\overline{u_{obs}}$, based on UKMO measurements at a height of 10m in an isolated environment, is used to estimate the wind speed at a height of 100m, u_{100}, using Equation S1 (based on [42]).

$$u_{100} = \overline{u_{obs}} \cdot \frac{ln\left[(100-d)/z_0\right]}{ln\left[(10-d)/z_0\right]} \tag{S1}$$

where d is the zero-plane displacement height (m) – equal to approximately 0.7 x the height of any obstacles in the vicinity, forming a pseudo horizontal plane (e.g. the tops of closely-packed buildings) – and z_0 is the surface roughness (m). UKMO stations are typically located in open terrain, free of obstacles (typically grassland) and we assume $d = 0$ m and $z_0 = 0.02$ m (see, e.g.,[72]), yielding Equation S2.

$$u_{100} = \overline{u_{obs}} \cdot \frac{ln(5000)}{ln(500)} \tag{S2}$$

Assuming the wind speed at a height of 100m above the street section is, to first order, similar to the wind speed at 100m above the nearest UKMO station, we can likewise use a log wind profile to estimate the wind speed at a height z (m) above the base of the street, u_z, according to Equation S3 (where z > d).

$$u_z = \overline{u_{obs}} \cdot \frac{ln(5000)}{ln(500)} \cdot \frac{ln\left[(z-d)/z_0\right]}{ln\left[(100-d)/z_0\right]} \tag{S3}$$

where d is the zero plane displacement height (m) and z_0 is the surface roughness (m) in that street environment. In practice, z_0 will vary from one street to another, but currently, for simplicity, we adopt a single value representative of suburban conditions, z_0= 0.2m [72]. In the absence of literature on the variation of d between streets of different aspect ratio, we assume that d is a function of building height (H) and street width (W), decreases linearly from 0.7H to 0 as W increases from 1.5H to 5H, according to Equation S4.

$$d = \begin{cases} 0.7\,H & | \quad H \le W \le 1.5H \\ H - 0.2W & | \quad 1.5H < W \le 5H \\ 0 & | \quad W > 5H \end{cases} \tag{S4}$$

For each row in the ventilation region, Equation S3 is used to calculate u_z at 10 evenly-spaced heights from the top to the bottom of that row (specifying a minimum value of u_z, approximately where z <= d), and the mean horizontal advection velocity is adopted. Vertical advection velocities are then calculated to supply the necessary mass fluxes to sustain those horizontal advection velocities and conserve mass. So, e.g., in Figure 3 in the main paper: air is drawn down in C3, from the background into R3 and, to a

diminishing extent, from R3 to R2, and from R2 to R1; air is forced up in C5, from R1 to R2, from R2 to R3, and finally up and out of R3.

The flow within the recirculation region is distinctly different to that in the ventilated region and cannot be calculated by a logarithmic approach below building heights. The recirculation of air due to the upwind building is described by [41] as driven by an intermittent jet which decays in strength exponentially as it reverses in direction and approaches the upwind building. However, this model framework cannot currently describe such processes and we opt for a crude approach to capture the general effects of slower and less organized recirculation of air. Instead, the rooftop wind speed, u_H (i.e., u_z, where z=H) is used to calculate the advection velocities in the recirculation region. The recirculation velocity is estimated to be one tenth of u_H, which is supported conceptually by slower flow structures identified in CFD models [e.g. 73] and numerical simulations [74]. However, it is accepted that this methodology could be greatly improved, such as by varying the recirculation speed based on aspect ratio [75], side ratio [76], or by applying [41]'s methodology, but this was not within the scope of the initial framework development. The advection velocity is adjusted to remove any dependence of the resulting mass flux on the height of the uppermost row and is then propagated around the boxes inside the recirculation region, converting between horizontal and vertical velocities so as to conserve mass (i.e., accounting for changes in height or length of the interface, across which the velocity is applied).

In the simulations that include barriers, we modify the advection velocities in the vicinity of any barrier in the ventilation region, with which we have aligned a division between columns (see section 2.1.2 of the main paper). The green arrows in Figure S11 illustrate the modified flow of air when a barrier is introduced between boxes R1C3 and R1C4. In the current implementation, the horizontal advection velocity from R1C3 to R1C4 (through the barrier) is simply reduced linearly by the percentage obstruction posed by the barrier. The relationship between apparent obstruction (i.e., optical porosity), and the fraction of air forced around the barrier, is likely more complex and will be a focus of future development. To conserve mass, the horizontal advection velocity from R1C4 to R1C5 is likewise reduced, and so too are the vertical advection velocities from R2C3 to R1C3, and from R1C5 to R2C5. The reduced mass flux from left to right in the lowermost row, however, is compensated for by an increased mass flux from left to right in the middle row (over the barrier) from R2C3 to R2C4, and from R2C4 to R2C5. In the example illustrated in Figure S11, the extent of the partially isolated region of air in the immediate wake of the barrier (given by Equation 2 in the main paper) is marked by the division between columns C4 and C5. Where the street section allows us to include two columns beyond this region, the additional mass flux in the middle row is returned to the lowermost row in C4 before being forced up and out of the street in C5.

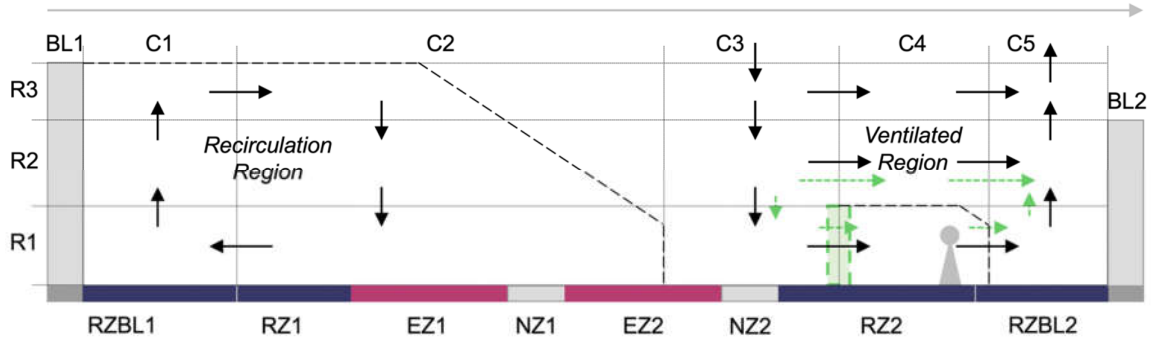

Figure S11 Example model grid and advection velocities when the wind aloft blows from left to right, in which the solid black (dashed green) arrows indicate the advection velocities used to simulate the flow of air in the absence (presence) of the proposed barrier (dashed green rectangle).

It is less clear if, and how, we should alter the advection velocities in the vicinity of a barrier within a recirculation region (e.g. when our example street section is subject to a

wind aloft blowing from right to left; see Figure S10 in SM section 4). Here, the advection velocities describing the circulation of air are typically an order of magnitude lower than those in the ventilated region [41], and already a simplified representation of the more complex patterns of air motion therein; in real streets, the circulation may be disturbed by even relatively small-scale architectural features, like balconies, and obstacles, such as parked cars (see, e.g., [44]) whilst moving vehicles draw air along the street (orthogonal to the recirculation) and create turbulence in their wake (see, e.g., [67]; [68]; and [69]). We opt – for the purposes of this prototype software – not to modify the advection velocities within the recirculation region, but simply to reduce the mixing of air between boxes either side of the barrier as outlined in the next section.

6. Estimating exchange velocities

The relatively slow exchange of pollutants between neighbouring boxes, as a result of turbulent mixing, is described by exchange velocities. We must ascribe an exchange velocity to each side of each box (except those marking the edge of buildings, or the ground, that are set to zero) in both perpendicular and parallel wind scenarios. We estimate these as follows.

When the wind aloft blows largely perpendicular to the street, the horizontal or vertical exchange velocity at each interface is simply assumed to be equal to one tenth of the horizontal or vertical advection velocity at that interface (estimated as outlined in SM section 5); the turbulent component is approximately an order of magnitude smaller than the mean flow component (e.g. [77]).

When the wind aloft blows predominantly parallel with the street, we assume: the exchange velocity between adjacent rows is equal to one tenth of the advection velocity along the street (not otherwise used in the model's calculations) at the height of the interface between those rows; and the exchange velocities between adjacent boxes within a row are equal to one tenth of the average advection velocity along the street at ten evenly-spaced heights between the top and bottom of that row. The advection velocity along the street is first estimated at the height of the lowermost building, in an analogous fashion to the rooftop wind speed, u_H, under perpendicular wind conditions: i.e., according to Equation S3 in SM section 5, where z=H but, this time, assuming zero displacement height, d=0 (irrespective of the street's aspect ratio) and $\overline{u_{obs}}$ is the time-averaged parallel component of the wind velocity when the wind blows within 45° of parallel to the street (based on 10 years of hourly observations from the nearest UKMO station, at which we have MIDAS-Open data [45]). We then assume that the advection velocity along the street decreases linearly – below the height of the lowermost building – to zero at the base of the street, similar to the 0° 'longitudinal' wind velocity profile simulated by [74] (see their Figure 11b).

Where the advection velocity across an interface is equal to zero, the exchange velocity is equated to the average of exchange velocities across nearby interfaces. For example, in Figure S11 in SM section 5, the exchange velocity between R2C4 and R3C4 is set to the average of the exchange velocities across the R3C3-R2C3 and R2C5-R3C5 interfaces. However, where interfaces distinguish between the recirculation region and the ventilated region, the exchange velocities are set to one hundredth of the rooftop windspeed, u_H (i.e., approximately one tenth of the advection velocity describing the recirculation; see SM section 5).

In the simulations that include barriers, we modify the exchange velocity at each interface aligned with a barrier, reducing the velocity by the percentage obstruction posed by that barrier; we do so for barriers aligned with interfaces within both the recirculation region and the ventilation region.

7. Mass conservation solver

The concentrations in every box at steady state are calculated from the relationship between the advection velocities, exchange velocities, and 'emission' fluxes. 'Emission' fluxes refer to all inflows or outflows of pollutants and therefore includes: direct emissions from vehicles, pollutants entering the street from air above the buildings, and pollutants exiting the street to the air above the building tops.

The concentration of pollutants for each box is represented by the vector $\vec{C}$, as described in Equations S5a and S5b:

$$\vec{C} = (C_1, C_2, C_3) \tag{S5a}$$

$$\vec{C} = (c_{11}, c_{12}, c_{13}, c_{14}, c_{15}, c_{21}, c_{22}, c_{23}, c_{24}, c_{25}, c_{31}, c_{32}, c_{33}, c_{34}, c_{35}) \tag{S5b}$$

Where C_1 in S5a refers to concentrations in row 1 and all columns. This can be expanded further to S5b, where c_{ij} refers to the concentration in box c of row i and column j. Meanwhile the 'emissions' can be described by vector $\vec{D}$, as described in Equations S6a and S6b:

$$\vec{D} = (D_1, D_2, D_3) \tag{S6a}$$

$$\vec{D} = (e_{11}, e_{12}, e_{13}, e_{14}, e_{15}, 0, 0, 0, 0, 0, w_{41}c_B, w_{42}c_B, w_{43}c_B, w_{44}c_B, w_{45}c_B) \tag{S6b}$$

Where D_1 in S6a refers to the inflows in row 1 and all columns. This can be expanded further to S6b where e_{ij} refers to the emissions into boxes of the first row (i) and each column (j). Vehicle emissions are limited to the first row in any scenario. The second row does not contain any direct emissions or influence from air above the tallest building and are therefore set to 0. The third row is influenced by inflows from the air above of background concentration (c_B) based on the exchange velocity across the uppermost interfaces w_{ij}. For mass to be conserved in steady state, the relationship between fluxes at interfaces (A), concentrations ($\vec{C}$), and inputs ($\vec{D}$), can be described by Equation S7:

$$A\vec{C} = \vec{D} \tag{S7}$$

Which can be expanded using S5a and S6a, and written according to Equation S8:

$$\begin{bmatrix} A_{11} & A_{12} & 0 \\ A_{21} & A_{22} & A_{23} \\ 0 & A_{32} & A_{33} \end{bmatrix} \begin{bmatrix} C_1 \\ C_2 \\ C_3 \end{bmatrix} = \begin{bmatrix} D_1 \\ D_2 \\ D_3 \end{bmatrix} \tag{S8}$$

Where the exchange and advection velocities across rows 1 and 2 (A_{11} and A_{12}) and concentrations in row 1 (C_1) are equal to the inputs in row 1 (D_1). Additionally, the exchange and advection velocities in row 1, 2, and 3 (A_{21}, A_{22} and A_{23}) and concentrations in row 2 (C_2) are equal to the inputs in row 2 (D_2). Finally, the exchange and advection velocities across rows 2 and 3 (A_{32} and A_{33}) and concentrations in row 3 (C_3) are equal to the inputs in row 3 (D_3). Note: subscripts of A refer to matrix positions and therefore do not directly correspond with box number notation. Equation S8 can also be written according to Equations S9-11.

$$A_{11}C_1 + A_{12}C_2 + 0 = D_1 \tag{S9}$$

$$A_{21}C_1 + A_{22}C_2 + A_{23}C_3 = D_2 \tag{S10}$$

$$0 + A_{32}C_2 + A_{33}C_3 = D_3 \tag{S11}$$

The A_{xy} matrices and the vector concentrations for each row (C_i) can be further expanded to give Equations S12-14:

$$\begin{bmatrix} a_{11} & a_{12} & 0 & 0 & 0 \\ a_{21} & a_{22} & a_{23} & 0 & 0 \\ 0 & a_{32} & a_{33} & a_{34} & 0 \\ 0 & 0 & a_{43} & a_{44} & a_{45} \\ 0 & 0 & 0 & a_{54} & a_{55} \end{bmatrix}\begin{bmatrix} C_{11} \\ C_{12} \\ C_{13} \\ C_{14} \\ C_{15} \end{bmatrix} + \begin{bmatrix} a_{16} & 0 & 0 & 0 & 0 \\ 0 & a_{27} & 0 & 0 & 0 \\ 0 & 0 & a_{38} & 0 & 0 \\ 0 & 0 & 0 & a_{49} & 0 \\ 0 & 0 & 0 & 0 & a_{510} \end{bmatrix}\begin{bmatrix} C_{11} \\ C_{12} \\ C_{13} \\ C_{14} \\ C_{15} \end{bmatrix} = D_1 \quad \text{(S12)}$$

$$\begin{bmatrix} a_{61} & 0 & 0 & 0 & 0 \\ 0 & a_{72} & 0 & 0 & 0 \\ 0 & 0 & a_{83} & 0 & 0 \\ 0 & 0 & 0 & a_{94} & 0 \\ 0 & 0 & 0 & 0 & a_{105} \end{bmatrix}\begin{bmatrix} C_{21} \\ C_{22} \\ C_{23} \\ C_{24} \\ C_{25} \end{bmatrix} + \begin{bmatrix} a_{66} & a_{67} & 0 & 0 & 0 \\ a_{76} & a_{77} & a_{78} & 0 & 0 \\ 0 & a_{87} & a_{88} & a_{89} & 0 \\ 0 & 0 & a_{98} & a_{99} & a_{910} \\ 0 & 0 & 0 & a_{109} & a_{1010} \end{bmatrix}\begin{bmatrix} C_{21} \\ C_{22} \\ C_{23} \\ C_{24} \\ C_{25} \end{bmatrix} + \begin{bmatrix} a_{611} & 0 & 0 & 0 & 0 \\ 0 & a_{712} & 0 & 0 & 0 \\ 0 & 0 & a_{813} & 0 & 0 \\ 0 & 0 & 0 & a_{914} & 0 \\ 0 & 0 & 0 & 0 & a_{1015} \end{bmatrix}\begin{bmatrix} C_{21} \\ C_{22} \\ C_{23} \\ C_{24} \\ C_{25} \end{bmatrix} = D_2 \quad \text{(S13)}$$

$$\begin{bmatrix} a_{116} & 0 & 0 & 0 & 0 \\ 0 & a_{127} & 0 & 0 & 0 \\ 0 & 0 & a_{138} & 0 & 0 \\ 0 & 0 & 0 & a_{149} & 0 \\ 0 & 0 & 0 & 0 & a_{1510} \end{bmatrix}\begin{bmatrix} C_{31} \\ C_{32} \\ C_{33} \\ C_{34} \\ C_{35} \end{bmatrix} + \begin{bmatrix} a_{1111} & a_{1112} & 0 & 0 & 0 \\ a_{1211} & a_{1212} & a_{1213} & 0 & 0 \\ 0 & a_{1312} & a_{1313} & a_{1314} & 0 \\ 0 & 0 & a_{1413} & a_{1414} & a_{1415} \\ 0 & 0 & 0 & a_{1514} & a_{1515} \end{bmatrix}\begin{bmatrix} C_{31} \\ C_{32} \\ C_{33} \\ C_{34} \\ C_{35} \end{bmatrix} = D_3 \quad \text{(S14)}$$

Where the a_{xy} term is determined by the advection and exchange velocities at each interface. The calculation of these values can be found in the Python code available at the GitHub repository (https://github.com/GI4RAQ/GI4RAQ-open) under the function called a_matrix. Alpha and beta functions are used to ensure the correct sign (+/-) is applied to each term. The methodology used to derive these equations can be provided upon request.